

The devil is in the details: Enhancing Video Virtual Try-On via Keyframe-Driven Details Injection

Qingdong He^{1*} Xueqin Chen^{2*} Yanjie Pan³ Peng Tang¹ Pengcheng Xu⁴ Zhenye Gan¹
 Chengjie Wang¹ Xiaobin Hu¹ Jiangning Zhang¹ Yabiao Wang¹

¹Tencent YouTu Lab ²Sichuan University ³Fudan University ⁴Western University

<https://huggingface.co/datasets/zijiyingcai/ViT-HD>



Figure 1. KeyTailor enables generating realistic and natural try-on videos with fine-grained consistency in both garment and background under challenging scenarios.

Abstract

Although diffusion transformer (DiT)-based video virtual try-on (VVT) has made significant progress in synthesizing realistic videos, existing methods still struggle to capture fine-grained garment dynamics and preserve background integrity across video frames. They also incur high computational costs due to additional interaction modules introduced into DiTs, while the limited scale and quality of existing public datasets also restrict model generalization and effective training. To address these challenges, we propose a novel framework, **KeyTailor**, along with a large-scale, high-definition dataset, **ViT-HD**. The core idea of KeyTailor is a keyframe-driven details injection strategy, motivated by the fact that keyframes inherently contain both fore-

ground dynamics and background consistency. Specifically, KeyTailor adopts an instruction-guided keyframe sampling strategy to filter informative frames from the input video. Subsequently, two tailored keyframe-driven modules—the garment details enhancement module and the collaborative background optimization module—are employed to distill garment dynamics into garment-related latents and to optimize the integrity of background latents, both guided by keyframes. These enriched details are then injected into standard DiT blocks together with pose, mask, and noise latents, enabling efficient and realistic try-on video synthesis. This design ensures consistency without explicitly modifying the DiT architecture, while simultaneously avoiding additional complexity. In addition, our dataset ViT-HD comprises 15,070 high-quality video samples at a resolution of 810×1080 , covering diverse garments. Extensive experiments demonstrate that KeyTailor outperforms state-of-the-

*Equal contribution.

art baselines in terms of garment fidelity and background integrity across both dynamic and static scenarios.

1. Introduction

The goal of video virtual try-on (VVT) is to generate natural, high-fidelity videos by substituting the clothing worn by the main character with a user-specified target garment image, while maintaining motion and visual consistency across consecutive frames. This technology not only addresses the challenge of online garment fitting for consumers on e-commerce platforms but also offers a novel and engaging experience for users on short-video platforms, making VVT an attractive direction for both industry applications and academic research.

Owing to the successful deployment of diffusion models in video generation [2, 20, 35], recent efforts in VVT increasingly employ diffusion models as their generator [13, 15, 25, 29, 36, 41]. These pioneers typically consist of a garment reference branch alongside a generation branch. The garment branch is responsible for extracting clothing appearance features and then interacting with the main generation branch through a tailored attention mechanism, thereby ensuring spatiotemporal consistency across frames. Although such approaches have achieved significant results, they are limited by the representational capacity of the U-Net-based [33] backbone, especially when it comes to rendering complex textures and details in human motions and garment appearance [22]. To overcome this limitation, recent studies [9, 22, 47] utilize large-scale video diffusion transformers (DiTs) [30] in place of the U-Net backbone. This alternative not only enhances the expressiveness and scalability of the network but also enables the joint modeling of temporal and spatial patterns, thereby resulting in more consistent video generation. However, such methods still face the following challenges:

(1) **Insufficient Garment Dynamic Details:** Although existing DiT-based methods introduce additional encoding components to learn garment appearance from both textual descriptions and visual inputs, they still fail to fully capture garment dynamic details across consecutive frames. Fine-grained cues such as backside textures, wrinkles caused by body motion (*e.g.*, raising an arm), and subtle lighting-dependent variations are often missing. As illustrated in Fig. 2(a), the SOTA method produces results with an incorrect belt position for the dress, and the generated video frames fail to capture garment variations induced by human motion (first row). In the third row, the generated garment size does not accurately correspond to the reference. These issues lead to over-smoothed garment appearances and insufficient fidelity compared to real-world dynamics.

(2) **Inconsistency of Background Areas:** Current methods solely rely on garment-agnostic videos to provide back-

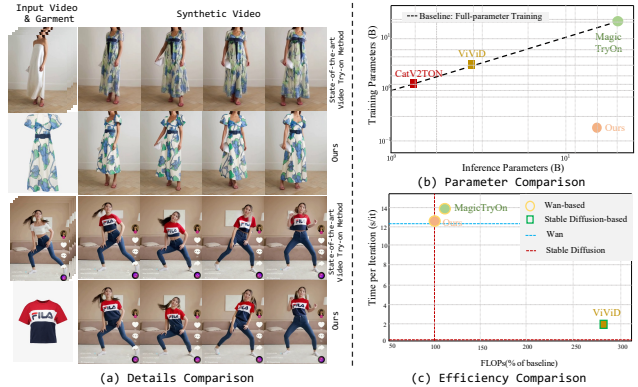


Figure 2. (a) Comparison of garment details; (b) Comparison of background details; (c) Comparison of parameters and efficiency.

ground conditions for video synthesis. However, this approach often results in (a) detail loss, where fine textures such as object patterns or edges are blurred; (b) temporal inconsistency, where elements vary unnaturally across consecutive frames, producing artifacts; and (c) environmental incoherence, where background structures deviate from the original video. For example, as shown in Fig. 2(a), the floor textures generated by the SOTA method are blurred (1st row); hair contours are inconsistent across frames, and the white frame on the wall does not align with the ground truth (3rd row). Hence, the synthesized video exhibits incoherence between garment regions and the background, and further fails to maintain background integrity, leading to degraded realism.

(3) **Increased Model Complexity and Data Scarcity:** To enhance generation conditions, existing paradigms typically incorporate additional interaction modules into the DiT backbone. While these components improve conditioning expressiveness, they also substantially increase model complexity and computational cost. As illustrated in Fig. 2(b) and Fig. 2(c), we visualize the parameter counts and efficiency of SOTA methods. It is evident that SOTA methods introduce a large number of additional parameters and significantly increase training costs. In addition, currently available open-source datasets (VVT [11] and ViViD [13]) remain limited in both scale and quality. Each consists of only a few thousand short clips, often with low resolution, simple backgrounds, and limited garment diversity. These constraints prevent DiT-based methods from fully leveraging their expressive power, hindering generalization to complex scenarios and restricting high-resolution video generation.

To address the lack of fine-grained details and reduce computational cost, we propose a novel DiT-based framework, KeyTailor, built on a keyframe-driven details injection strategy. This design is motivated by the fact that informative keyframes inherently capture multi-view gar-

ment dynamics and subtle background information, which can be utilized to improve garment fidelity and background integrity. Specifically, KeyTailor employs an instruction-guided keyframe sampling approach to select frames that capture view and motion variations. This is followed by two lightweight, keyframe-driven modules for details enrichment: a garment dynamics details enhancement module, which enriches multi-view garment dynamic details (e.g., wrinkles and texture variations), and a collaborative background details optimization module, which preserves structural integrity and semantic consistency in background regions. The enriched details are then fused with other conditions (e.g., pose and mask latents) and injected into DiTs for realistic video synthesis. As illustrated in both Fig. 1 and Fig. 2(a), our KeyTailor ensures consistent garment dynamics and background integrity across all frames, resulting in more natural video synthesis. Importantly, KeyTailor is built upon standard DiTs without introducing additional interaction layers, and these are fine-tuned with a LoRA adapter, thereby reducing computational demand, as evidenced by Fig. 2(b) and Fig. 2(c). In addition, to combat data scarcity, we self-collect a large-scale dataset from multiple e-commerce platforms, containing 15,070 high-quality samples at a resolution of 810×1080 , to facilitate training and evaluation. In summary, the contributions of this work are as follows:

- We propose KeyTailor, a novel DiT-based framework that adopts a keyframe-driven details injection strategy to enhance garment fidelity and background integrity, without introducing additional interaction layers into the DiT backbone.
- We design an instruction-guided keyframe sampling approach to select informative keyframes, along with two lightweight keyframe-driven details injection modules—a garment dynamic details enhancement module and a collaborative background details optimization module—to ensure that the details injected into DiTs provide sufficient garment fidelity and background integrity.
- We curate ViT-HD, a new large-scale and high-definition dataset collected from multiple e-commerce platforms, containing 15,070 video samples at a resolution of 810×1080 , across various garment styles.
- We conduct extensive experiments on ViT-HD, as well as on two widely used VVT datasets and two image-based virtual try-on datasets, demonstrating that KeyTailor outperforms state-of-the-art baselines in both garment fidelity and background consistency across dynamic and static scenarios.

2. ViT-HD Dataset

Existing public datasets, VVT [11] and ViViD [13], either suffer from extremely low resolution—resulting in the loss of fine-grained garment textures and details—or are restricted

Table 1. Dataset Comparison. We compare our ViT-HD with existing video virtual try-on datasets along four dimensions: resolution, garment diversity (multi-class), video content quality (no start-frame overexposure and intact subject integrity), and data scale.

Datasets	Resolution	Multi Class	No Start Overexposure	Subject Integrity	Scale
VVT	192×256	×	✓	×	791
ViViD	632×824	✓	×	×	9,700
ViT-HD	810×1080	✓	✓	✓	15,070

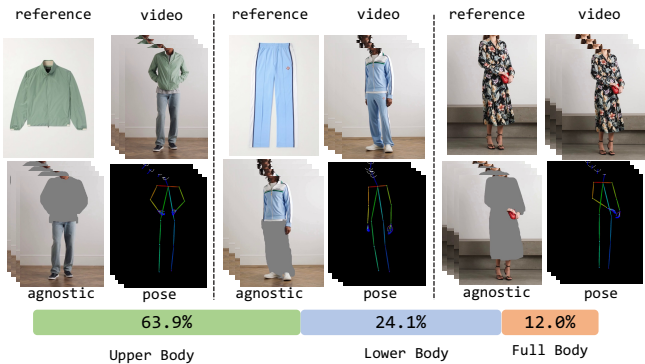


Figure 3. Dataset overview.

to simple, repetitive runway scenes. Moreover, their limited scale still falls short of the growing need for large, high-quality video data. To address these limitations, we curate a new dataset, ViT-HD, which significantly expands both the scale and quality of available resources. Table 1 provides a detailed comparison between our dataset and existing ones. Our proposed ViT-HD contains 15,070 samples featuring diverse garment styles, each with a resolution of 810×1080 .

Data collection and processing: Our raw data are collected from multiple e-commerce platforms in compliance with their respective terms of service. In addition, we filter out all sensitive information to further mitigate potential copyright concerns. Each raw data sample consists of a high-resolution garment image together with a corresponding high-definition model showcase video, both cropped at a resolution of 1080×810 . Then, for each raw data sample, we follow ViViD [13] to extract its pose video and masked video. Specifically, we employ OpenPose [3] to detect skeletal keypoints and generate pose sequences. To obtain masked videos, we adopt the same segmentation pipeline as OOTDiffusion [40]. For each frame, we utilize OpenPose [3] together with HumanParsing [24] to infer body-part masks and create a garment-agnostic background image by inpainting the clothed regions. The resulting frames are then post-processed and stitched together to form the masked video. Furthermore, we categorize each data sample into one of three types—upper-body, lower-body, or full-

body outfits—using BLIP-2 [23]. During the data processing stage, we discard videos that contain a large number of frames with incomplete clothing occlusion to preserve subject integrity. In addition, we remove overexposed frames at the beginning of the original videos to maintain consistent color tones across all frames within each video. Fig. 3 presents an overview of ViT-HD.

3. Method

Our KeyTailor is built upon diffusion transformers (DiTs), aiming to provide a lightweight solution for synthesizing realistic, high-fidelity videos that capture dynamic garment details while maintaining background consistency. To this end, we propose a keyframe-driven details injection strategy with two tailored feature extraction modules: a *garment dynamics enhancement module* and a *collaborative background optimization module*. Specifically, these two modules strengthen garment dynamics and background integrity by leveraging information from keyframes as supplementary input. The enriched fine-grained details are then directly injected into DiTs to introduce multi-view garment variations and preserve background consistency—without explicitly introducing interaction modules into the DiT architecture, as required in prior work [9, 22, 47]. The overall framework of KeyTailor is illustrated in Fig. 4.

3.1. Keyframe-driven Details Injection

The goal of VVT is to synthesize a new video by replacing the clothing worn by a character, while preserving all other aspects—such as motion, background, and garment dynamics—consistent with the original video. We argue that keyframes naturally capture critical information about both garment variations and background consistency, making them highly beneficial for guiding DiTs. Based on this assumption, we propose a keyframe-driven details injection strategy. This strategy is implemented through an instruction-guided keyframe sampling module and two lightweight keyframe-driven injection modules: a garment dynamic details enhancement module and a collaborative background details optimization module.

Instruction-guided keyframe sampling. Effectively selecting informative keyframes is the key to our keyframe-driven details injection. To ensure that the selected frames adequately capture both view changes (*e.g.*, front and back) and action changes (*e.g.*, raising a hand) from V_{in} , we propose an instruction-guided keyframe sampling module (IKS). IKS first employs a large visual-language model (*e.g.*, QWen [1]) to parse the predefined view–action instruction and extract the target views \mathcal{V}_{tar} and actions \mathcal{A}_{tar} , which reflect view variation and action dynamics, respectively. Then, IKS applies HumanParsing [24] to generate standardized multi-anchor pose frames F_{anc} corresponding to \mathcal{V}_{tar} and \mathcal{A}_{tar} . Subsequently, for each frame $f \in V_{in}$, IKS

computes a motion-difference score $S_m(f)$ with respect to F_{anc} , along with a garment-area ratio score $S_r(f)$ (see Appendix C for details). The final score of the frame f is computed as follows:

$$S_f(f) = 1 - S_m(f) + \lambda \cdot S_r(f), \quad (1)$$

where λ is a balancing coefficient. Next, all frames are sorted in descending order according to their S_f . Rather than simply selecting the top- k frames to construct the final multi-view keyframes F_{key} , we adopt a dual-selection strategy to reduce redundancy and ensure temporal uniformity. Specifically, two thresholds are defined to constrain both the score difference and the temporal interval between the current frame f and candidate frames $f_{key} \in F_{key}$. The pseudo-code for this procedure is provided in Appendix G. **Garment Dynamic Details Enhancement.** Unlike previous works that learn garment appearance solely by embedding the garment image I_{ref} or incorporating textual descriptions, our garment dynamic details enhancement module (GDDE) instead encodes the edited first-frame result and further enriches it with features extracted from keyframes. Specifically, GDDE first crops the initial frame f_{agn}^0 from the agnostic video V_{agn} , and employs a pre-trained single-image try-on model with LoRA [16] layers to inject the garment appearance into f_{agn}^0 . The resulting try-on frame is then projected into a latent representation L_g using a pre-trained VAE-based image encoder \mathcal{E}_{VAE} . Then, GDDE enriches L_g with fine-grained garment variations derived from F_{key} , such as backside textures and wrinkles caused by raised arms. It first extracts garment-specific features L_{key}^{gar} from F_{key} by encoding the garment regions of each keyframe using \mathcal{E}_{VAE} , where the garment regions are obtained through the segmentation operation. Subsequently, GDDE employs a lightweight distillation component \mathcal{D} to inject garment variation details from L_{key}^{gar} into L_g . The formulation is shown as follows:

$$\bar{L}_g = \mathcal{D}(\text{Concat}(L_g, \frac{1}{|F_{key}|} \sum_{L_k \in L_{key}^{gar}} L_k)). \quad (2)$$

Here, \mathcal{D} is implemented using two 1×1 convolution layers followed by a LayerNorm layer.

Collaborative Background Details Optimization. Preserving background integrity is crucial for synthesizing realistic video scenes. Existing methods typically encode the garment-agnostic video V_{agn} into a latent representation as the background condition for DiTs. However, since V_{agn} is generated by applying image inpainting to each frame of the original video to fill in garment regions, it inevitably loses subtle background details. To this end, we design a collaborative background details optimization module (CBDO), which introduces keyframes as supplementary cues to enrich the semantics of V_{agn} . Specifically, CBDO consists of

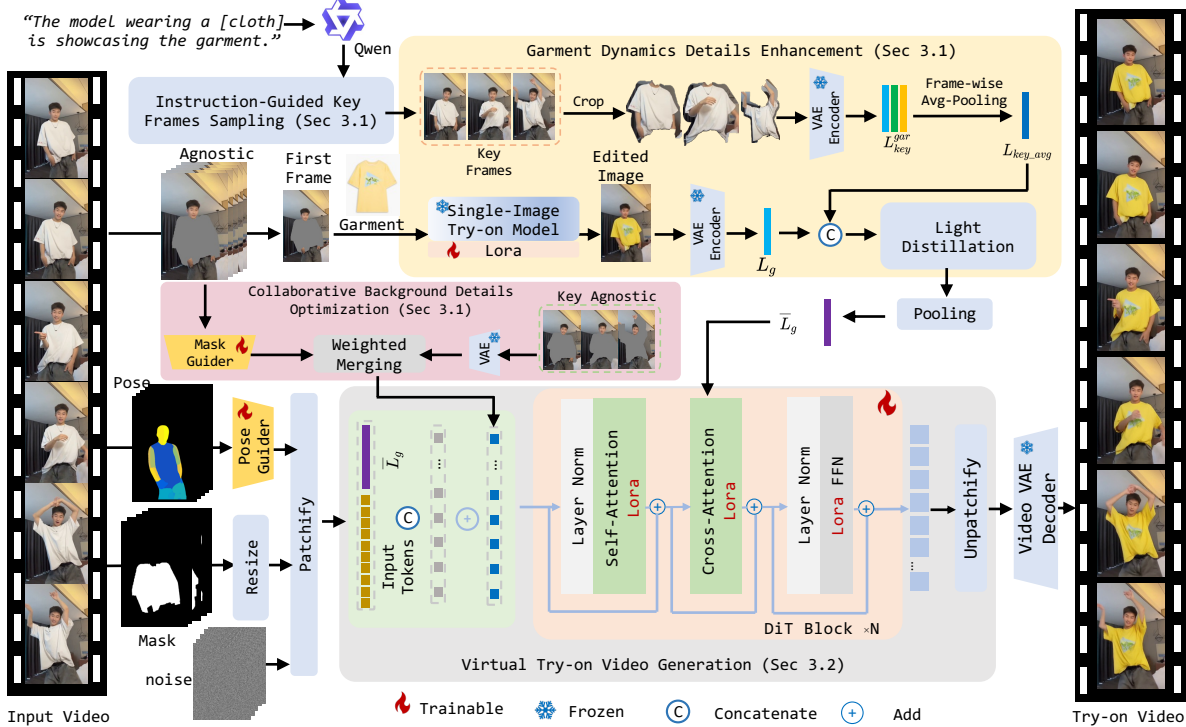


Figure 4. **Overall framework of KeyTailor.** KeyTailor takes as input a reference garment image I_{ref} , a source video V_{in} , its corresponding agnostic video V_{agn} , agnostic masks M_{agn} , and pose representations P . These inputs are encoded into garment-related latents L_g , background-related latents L_{bg} , pose latents L_p , and resized masks L_m . Specifically, garment-related latents are generated by the GDDE module, background-related latents by the CBDO module, and pose latents by a trainable pose guider. Subsequently, all these latents, together with noise latents, are injected into N DiT blocks to produce the final try-on video tokens, which are then decoded by a VAE-based video decoder to synthesize the output video.

two branches: a *coarse global background encoding branch* and a *fine-grained keyframe-driven local detail enrichment branch*. In the first branch, CBDO employs a mask guider \mathcal{E}_{BG} to project V_{agn} into a latent representation L_{bg} , thereby capturing the global structural layout and semantic context of the background. \mathcal{E}_{BG} is implemented with four 3D convolutional layers, having channel dimensions of 32, 96, 192, and 256, respectively. To facilitate smoother latent guidance during video synthesis training, the linear layer in \mathcal{E}_{BG} is zero-initialized. In the second branch, CBDO extracts subtle background details from keyframes. Specifically, it first crops the background regions using an inverse human-body mask operation and then encodes them into latent representations with \mathcal{E}_{VAE} , denoted as L_{key}^{bg} . To avoid redundancy and ambiguity in fine-grained background details, we select only the frame with the highest background completeness score as the supplementary input to L_{bg} , yielding the enhanced background latents:

$$\bar{L}_{bg} = \alpha \cdot L_{bg} + (1 - \alpha)L_{key}^{max}, \quad (3)$$

where α is a balance weight, with a default setting to 0.3.

3.2. Virtual Try-on Video Generation

After obtaining the enhanced garment-related latents \bar{L}_g and optimized background-related latents \bar{L}_{bg} , we adopt a *three-step fusion strategy* rather than directly concatenating them with the pose latent L_p , the resized agnostic masks L_m , and the noise ϵ as input to the DiTs. First, L_p and L_m are concatenated and patchified into input tokens T_{inp} , which are then fused with \bar{L}_g through a projection layer \mathcal{R} to produce L . L is then concatenated with patchified ϵ to form \bar{L} . Finally, \bar{L}_{bg} is injected into \bar{L} via the “addto” operation, yielding the final guidance tokens for DiTs. In this way, the guidance preserves fine-grained background details while maintaining pose structure and garment dynamics. During the denoising step, we stack N DiT blocks and apply LoRA to finetune their attention modules, including both self-attention and cross-attention. Moreover, the garment-related latents \bar{L}_g is injected into the cross-attention component, substituting the original text tokens to mitigate the loss of garment details. Architecturally, KeyTailor only performs detail injection without modifying any component of the original DiT architecture, thereby avoiding the introduction of massive training parameters compared to prior works [22]. After several denoising iterations within the

DiT backbone, the network generates try-on video tokens, which are subsequently decoded into video sequences by the Video VAE decoder. The training details of KeyTailor are described in Appendix E.

4. Experiments

4.1. Setups: Datasets and Details

Datasets: We conduct experiments on our proposed dataset ViT-HD, as well as on the publicly available VVT [11] and ViViD [13] datasets. ViViD contains 7,759 paired video training samples, while ViT-HD provides 13,070 paired training samples and 2,000 test samples after partitioning. For training, we combine ViT-HD with ViViD, and for testing, we additionally evaluate on indoor scenarios using the ViViD-S and VVT datasets. To further assess generalization ability, we also perform experiments on two image-based virtual try-on datasets, VITON-HD [6] and DressCode [27].

Implementation Details: We adopt the pre-trained weights from Wan2.1-I2V-14B-720P as the base model. To address overexposure and subject loss in the opening frames of ViViD videos, we truncate the initial frames of each sequence. During training, each video sample consists of 81 frames, with a batch size of 1, and training is performed for 14,500 iterations. We use the AdamW optimizer with a fixed learning rate of $1e-4$. FiTDiT [17] is employed as the image-based virtual try-on model, following the official default settings. For video inference, the number of inference steps is set to 25. To ensure fairness, all model variants in the ablation studies are evaluated under the same hyperparameter configurations during inference.

4.2. Performance comparison with SOTA methods

Quantitative Comparison: Table 2 and Table 3 report the results of SOTA baselines and our KeyTailor for the video virtual try-on task on ViT-HD, VVT, and ViViD, respectively. It is evident that KeyTailor outperforms existing SOTA methods across nearly all metrics in both paired and unpaired settings. This demonstrates that KeyTailor achieves superior visual quality and temporal consistency in synthesized videos. We attribute this improvement to the injection of keyframe information, which provides both garment dynamics and subtle background details. Leveraging these cues enhances garment fidelity and preserves background integrity consistently across video frames. Notably, after fine-tuning on our dataset, the performance of KeyTailor on the ViViD dataset further improves (KeyTailor^S), whereas DreamVVT shows no comparable gain when trained on its own dataset. This suggests that our collected ViT-HD covers richer and more diverse scenarios. Additionally, the results on the image virtual try-on task (Table 4), show that KeyTailor also delivers better performance in static scenarios, further validating its gener-

alization ability.

Qualitative Comparison: We present the synthesized results of baselines and our method in Fig. 5 and Fig. 6. In Fig. 5, we visualize results on ViViD and our dataset, as well as an example under an in-the-wild scenario. It can be observed that KeyTailor not only preserves garment details but also maintains background consistency. Specifically, our method retains more garment details and patterns, adapts better to human motion, and produces more reasonable and natural fits, whereas other methods often lose details or even alter garment styles. Additionally, regions outside the garment remain more consistent with the original video in our results, exhibiting fewer artifacts and clearer background structures. In Fig. 6, we evaluate SOTA methods and our KeyTailor using a more challenging reference garment image, *i.e.*, person-to-video garment transfer. Our KeyTailor still preserves fine-grained garment details and maintains background consistency, demonstrating robust performance even under complex garment transfer scenarios.

Computational and Parameter Efficiency Analysis. We analyze the computational cost and parameter overhead of different baselines built upon various diffusion backbones, and also compare each method against its underlying backbone. All experiments are conducted on the ViViD dataset using 64-frame samples for consistency. The results are summarized in Table 5. Compared with its backbone, KeyTailor introduces only a 2.10% increase in parameters, which is substantially lower than the overhead brought by MagicTryOn (15.11%) and ViViD (157.10%). Since the base model of CatV2TON cannot be reproduced under consistent settings due to the removal of its text-attention layers, no reliable reference is available. Moreover, KeyTailor maintains computational demands comparable to Wan 2.1 (approximately 194K FLOPs and 12.58 s/it) while training on only 0.2057B parameters—significantly fewer than those required by MagicTryOn (16.446B).

User Study. We conduct a user study following the standard win-rate methodology to evaluate our approach. Each questionnaire contains 15 randomly selected generated videos presented in randomized order, and participants are asked to evaluate them along three dimensions: visual quality, semantic consistency, and overall quality. In total, we collect 80 completed feedback forms, with the results presented in Fig. 7. The majority of participants prefer our KeyTailor over SOTA methods, with particularly clear advantages compared to CatV2TON and ViViD. These findings demonstrate that our method produces more realistic, coherent, and user-preferred video try-on results.

4.3. Ablation Study

We conduct an ablation study by deactivating individual modules (see Appendix F for details) to demonstrate the ef-

Table 2. Quantitative Comparison of Video Virtual Try-On Results on our ViT-HD (*Left*) and VVT [11] (*Right*). The best and second-best results are marked with **red** and **blue**, respectively. p and u denote the paired setting and unpaired setting, respectively.

Methods	VFID $_I^p$ ↓	VFID $_{R^p}^p$ ↓	SSIM↑	LPIPS↓	VFID $_I^u$ ↓	VFID $_{R^u}^u$ ↓	Methods	VFID $_I^p$ ↓	VFID $_{R^p}^p$ ↓	SSIM↑	LPIPS↓
<i>Image-centered Method</i>							FW-GAN [11]	8.019	0.1215	0.675	0.283
StableVITON [19]	38.2686	0.8021	0.7986	0.1608	39.2286	0.8525	MV-TON [46]	8.367	0.0972	0.853	0.233
OOTDiffusion [40]	30.2521	4.0068	0.7925	0.1125	38.5214	5.5221	ClothFormer [18]	3.967	0.0505	0.921	0.081
CatVTON [8]	22.2365	0.4028	0.8156	0.1325	28.2065	0.7352	ViViD [13]	3.793	0.0348	0.822	0.107
<i>Video-centered Method</i>							CatV2TON [9]	1.778	0.0103	0.900	0.039
ViViD [13]	19.0568	0.7525	0.8022	0.1363	22.6856	0.7925	MagicTryOn [22]	1.991	0.0084	0.958	0.024
CatV2TON [9]	15.8725	0.2898	0.8545	0.0976	20.0187	0.5762	KeyTailor	1.226	0.0059	0.968	0.016
MagicTryOn [22]	14.0587	0.2461	0.8622	0.0828	19.2253	0.5587					

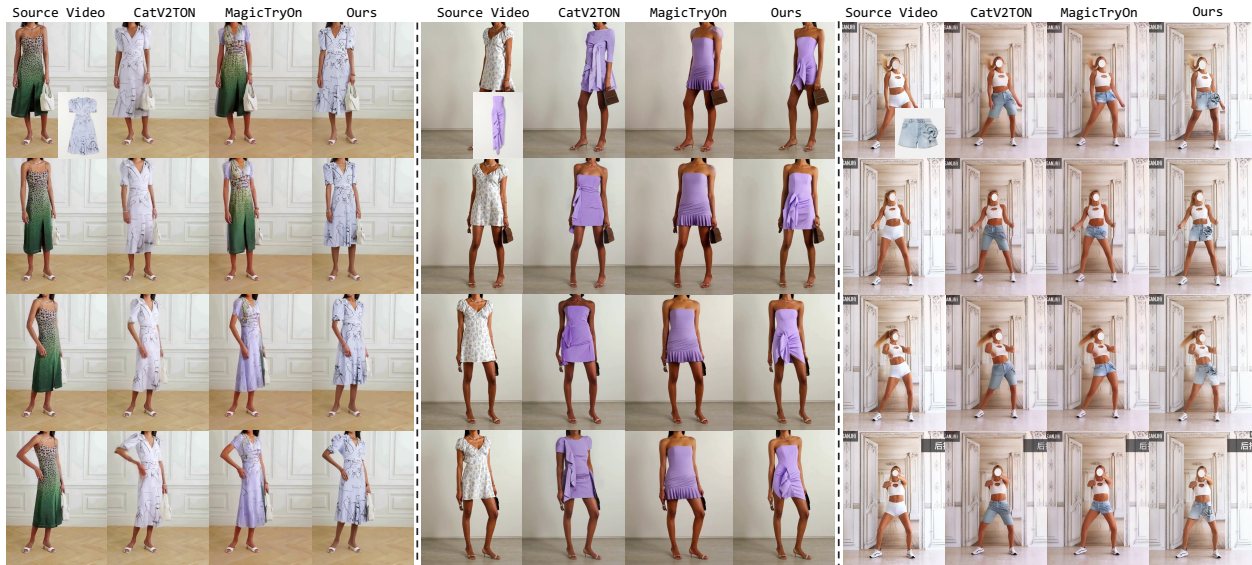


Figure 5. Qualitative comparison of video virtual try-on results on the ViViD dataset (1st column), our ViT-HD dataset (2nd column), and in-the-wild scenarios (3rd column). Our KeyTailor restores fine-grained garment details while preserving background integrity.

Table 3. Quantitative Comparison of Video Virtual Try-On Results on ViViD [13] dataset. § denotes methods that are additionally fine-tuned on their own proposed datasets, while all other methods are trained under a consistent setting.

Methods	VFID $_I^p$ ↓	VFID $_{R^p}^p$ ↓	SSIM↑	LPIPS↓	VFID $_I^u$ ↓	VFID $_{R^u}^u$ ↓
StableVITON [19]	34.2446	0.7735	0.8019	0.1338	36.8985	0.9064
OOTDiffusion [40]	29.5253	3.9372	0.8087	0.1232	35.3170	5.7078
IDM-VTON [7]	20.0812	0.3674	0.8227	0.1163	25.4972	0.7167
ViViD [13]	17.2924	0.6209	0.8029	0.1221	21.8032	0.8212
CatV2TON [9]	13.5962	0.2963	0.8727	0.0639	19.5131	0.5283
MagicTryOn [22]	12.1988	0.2346	0.8841	0.0815	17.5710	0.5073
DreamVVT [§] [47]	11.0180	0.2549	0.8737	0.0619	16.9468	0.4285
KeyTailor	9.5285	0.2761	0.8985	0.0585	14.5381	0.3869
KeyTailor[§]	8.2164	0.1854	0.9023	0.0522	14.1521	0.3106

effectiveness of each component in KeyTailor. The results are reported in Table 6. Overall, the full version of KeyTailor outperforms all variants. Removing any component leads to a clear performance degradation, with the garment

Table 4. Quantitative Comparison of Image Virtual Try-on Results on VITON-HD [6] and DressCode [27].

Metric	Methods								
	GP-V TON [36]	LaDI-V TON [28]	IDM-V TON [7]	OOT Diffusion [40]	CatV TON[8]	CatV2 TON[9]	Magic TryOn[22]	Key Tailor	
VITON-HD	FID p ↓	8.726	11.386	6.338	9.305	6.139	8.095	8.036	5.293
	KID p ↓	3.944	7.248	1.322	4.086	0.964	2.245	1.235	0.720
	SSIM ↑	0.8701	0.8603	0.8806	0.8187	0.8691	0.8902	0.8936	0.9201
	LPIPS ↓	0.0585	0.0733	0.0789	0.0876	0.0973	0.0572	0.0477	0.0566
	FID u ↓	11.844	14.648	9.611	12.408	9.143	11.222	8.696	8.528
	KID u ↓	4.310	8.754	1.639	4.689	1.267	2.986	1.130	0.788
DressCode	FID p ↓	9.927	9.555	6.821	4.610	3.992	5.722	5.428	2.746
	KID p ↓	4.610	4.683	2.924	0.955	0.818	2.338	1.078	0.517
	SSIM ↑	0.7711	0.7656	0.8797	0.8854	0.8922	0.9222	0.9572	0.9621
	LPIPS ↓	0.1801	0.2366	0.0563	0.0533	0.0455	0.0367	0.0271	0.0347
	FID u ↓	12.791	10.676	9.546	12.567	6.137	8.627	6.962	5.147
	KID u ↓	6.627	5.787	4.320	6.627	1.549	3.838	0.908	1.012

dynamics distillation (*w/o D*) showing the most significant drop. The results of “*w/o IKS*” and “ $F_{key} = 1$ ” demonstrate that the IKS module can accurately select informative frames and highlight the importance of using multiple keyframes. Fig. 8 provides an intuitive visual comparison, showing that removing these components results in

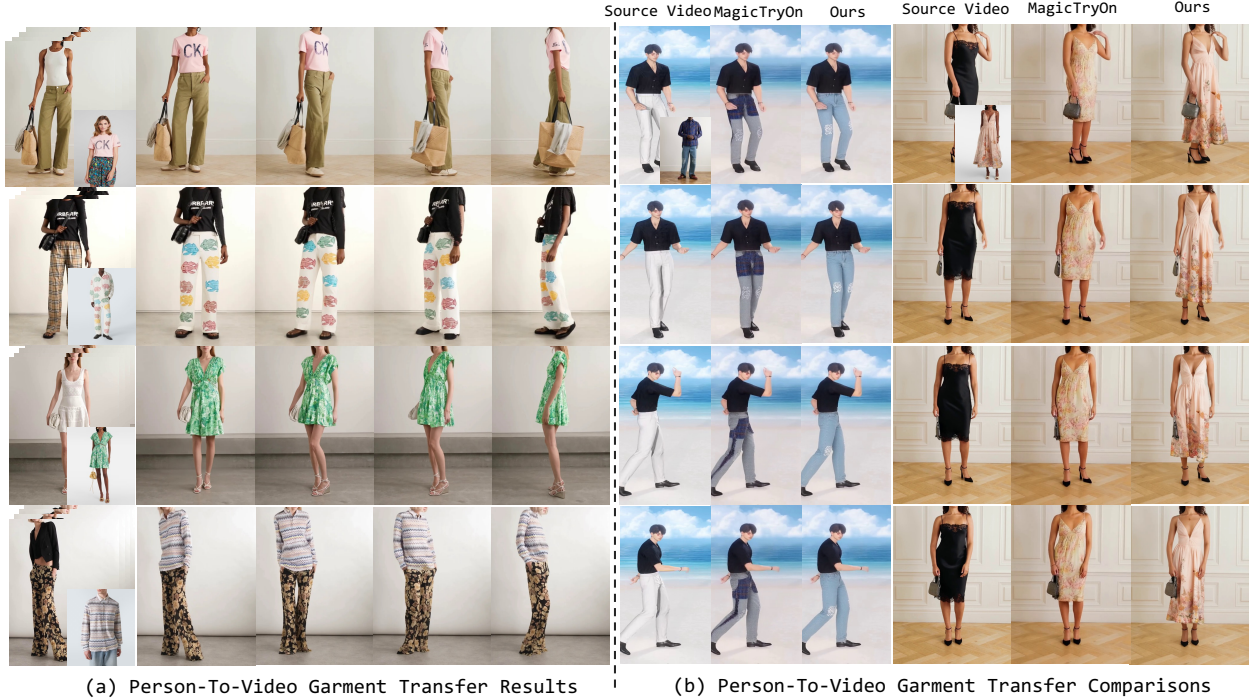


Figure 6. Qualitative results and comparisons in person-to-video garment transfer scenarios. Our method combines background, person, and garment more naturally in complex scenarios.

Table 5. Comparison of computational and parameter overhead. The first row per column is base model. Base model of CatV²TON not fairly reproducible due to removal of text attention layers.

Method	FLOPs (G)	s/fit	Params (B) Train / Infer	Inference Time (s)
Stable Diffusion 1.5 [32]	338.75	0.05	- / 0.8594	-
ViViD [13]	960.60	2.07	2.2093 / 2.2093	204.18
CatV2TON [9]	11672.00	1.04	1.3366 / 1.3366	209.13
Wan2.1 [35]	193899.00	12.38	- / 14.2860	-
MagicTryOn [22]	206934.73	13.69	16.4460 / 16.4460	345.27
KeyTailor	194607.28	12.58	0.2057 / 14.5866	281.65



Figure 7. User Study. We report pairwise preference rates from the perspectives of visual quality, semantic consistency, and overall quality.

noticeable generation errors, such as unnatural color shifts, distorted backgrounds, hallucinated objects, and skin tone changes.

More Ablation Studies and discussions are presented in the Appendix.

5. Conclusion

In this work, we present KeyTailor, a novel DiT-based video virtual try-on model, along with ViT-HD, a large-scale high-definition dataset. KeyTailor is designed based on a

Table 6. Ablation study of each component on the ViT-HD dataset.

Ablation Setting	VFID _T ^p ↓	VFID _R ^p ↓	SSIM↑	LPIPS↓	VFID _T ^u ↓	VFID _R ^u ↓
w/o IKS	16.2586	0.3568	0.8035	0.1022	21.6326	0.5679
w/o $S_r(f)$	17.2568	0.4566	0.8461	0.1125	22.0187	0.5602
w/o D	22.5241	0.5869	0.7658	0.2106	25.3632	0.7901
w/o Q_{key}	15.9878	0.8201	0.8569	0.0807	21.5855	0.6988
w/o L_{key}^{bg}	16.2526	0.6645	0.8622	0.0823	22.3523	0.8725
w/o Fusion	16.2885	0.6022	0.8254	0.0935	23.5525	0.8263
w/o CBDO	17.2134	0.7826	0.8523	0.0982	22.3965	0.6885
w/o GDDE	19.8968	0.5863	0.8429	0.1136	23.5662	0.8255
$F_{key} = 1$	16.3856	0.3988	0.8165	0.0987	21.8867	0.5969
KeyTailor	7.5267	0.1628	0.9066	0.0397	13.6628	0.3519



Figure 8. Qualitative comparison of KeyTailor with variants on ViT-HD.

keyframe-driven details injection strategy, implemented via an instruction-guided keyframe sampling module and two lightweight keyframe-driven details injection modules: the garment dynamic details enhancement and the collaborative

background details optimization. Extensive experiments on both video and image try-on tasks show that KeyTailor achieves superior garment fidelity, background integrity, and temporal consistency, establishing strong baselines and resources for future research in this field.

References

- [1] Jinze Bai, Shuai Bai, Yunfei Chu, Zeyu Cui, Kai Dang, Xiaodong Deng, Yang Fan, Wenbin Ge, Yu Han, Fei Huang, Binyuan Hui, Luo Ji, Mei Li, Junyang Lin, Runji Lin, Dayiheng Liu, Gao Liu, Chengqiang Lu, Keming Lu, Jianxin Ma, Rui Men, Xingzhang Ren, Xuancheng Ren, Chuanqi Tan, Sinan Tan, Jianhong Tu, Peng Wang, Shijie Wang, Wei Wang, Shengguang Wu, Benfeng Xu, Jin Xu, An Yang, Hao Yang, Jian Yang, Shusheng Yang, Yang Yao, Bowen Yu, Hongyi Yuan, Zheng Yuan, Jianwei Zhang, Xingxuan Zhang, Yichang Zhang, Zhenru Zhang, Chang Zhou, Jingren Zhou, Xiaohuan Zhou, and Tianhang Zhu. Qwen technical report. *arXiv preprint arXiv:2309.16609*, 2023. 4
- [2] Andreas Blattmann, Tim Dockhorn, Sumith Kulal, Daniel Mendelevitch, Maciej Kilian, Dominik Lorenz, Yam Levi, Zion English, Vikram Voleti, Adam Letts, et al. Stable video diffusion: Scaling latent video diffusion models to large datasets. *arXiv preprint arXiv:2311.15127*, 2023. 2, 12
- [3] Zhe Cao, Gines Hidalgo, Tomas Simon, Shih-En Wei, and Yaser Sheikh. Openpose: Realtime multi-person 2d pose estimation using part affinity fields. *IEEE transactions on pattern analysis and machine intelligence*, 43(1):172–186, 2019. 3
- [4] Joao Carreira and Andrew Zisserman. Quo vadis, action recognition? a new model and the kinetics dataset. In *proceedings of the IEEE Conference on Computer Vision and Pattern Recognition*, pages 6299–6308, 2017. 13
- [5] Chun-Fu Richard Chen, Quanfu Fan, and Rameswar Panda. Crossvit: Cross-attention multi-scale vision transformer for image classification. In *Proceedings of the IEEE/CVF international conference on computer vision*, pages 357–366, 2021. 12
- [6] Seunghwan Choi, Sunghyun Park, Minsoo Lee, and Jaegul Choo. Viton-hd: High-resolution virtual try-on via misalignment-aware normalization. In *Proceedings of the IEEE/CVF conference on computer vision and pattern recognition*, pages 14131–14140, 2021. 6, 7, 12
- [7] Yisol Choi, Sangkyung Kwak, Kyungmin Lee, Hyungwon Choi, and Jinwoo Shin. Improving diffusion models for authentic virtual try-on in the wild. In *European Conference on Computer Vision*, pages 206–235. Springer, 2024. 7
- [8] Zheng Chong, Xiao Dong, Haoxiang Li, Shiyue Zhang, Wenqing Zhang, Xujie Zhang, Hanqing Zhao, and Xiaodan Liang. Catvton: Concatenation is all you need for virtual try-on with diffusion models, 2025. 7
- [9] Zheng Chong, Wenqing Zhang, Shiyue Zhang, Jun Zheng, Xiao Dong, Haoxiang Li, Yiling Wu, Dongmei Jiang, and Xiaodan Liang. Catv2ton: Taming diffusion transformers for vision-based virtual try-on with temporal concatenation. *arXiv preprint arXiv:2501.11325*, 2025. 2, 4, 7, 8, 12
- [10] Hyung Won Chung, Noah Constant, Xavier Garcia, Adam Roberts, Yi Tay, Sharan Narang, and Orhan Firat. Unimax: Fairer and more effective language sampling for large-scale multilingual pretraining. *arXiv preprint arXiv:2304.09151*, 2023. 12
- [11] Haoye Dong, Xiaodan Liang, Xiaohui Shen, Bowen Wu, Bing-Cheng Chen, and Jian Yin. Fw-gan: Flow-navigated warping gan for video virtual try-on. In *Proceedings of the IEEE/CVF international conference on computer vision*, pages 1161–1170, 2019. 2, 3, 6, 7, 12
- [12] Patrick Esser, Sumith Kulal, Andreas Blattmann, Rahim Entezari, Jonas Müller, Harry Saini, Yam Levi, Dominik Lorenz, Axel Sauer, Frederic Boesel, et al. Scaling rectified flow transformers for high-resolution image synthesis. In *Forty-first international conference on machine learning*, 2024. 12
- [13] Zixun Fang, Wei Zhai, Aimin Su, Hongliang Song, Kai Zhu, Mao Wang, Yu Chen, Zhiheng Liu, Yang Cao, and Zheng-Jun Zha. Vivid: Video virtual try-on using diffusion models. *arXiv preprint arXiv:2405.11794*, 2024. 2, 3, 6, 7, 8, 12
- [14] Kensho Hara, Hirokatsu Kataoka, and Yutaka Satoh. Can spatiotemporal 3d cnns retrace the history of 2d cnns and imagenet? In *Proceedings of the IEEE conference on Computer Vision and Pattern Recognition*, pages 6546–6555, 2018. 13
- [15] Zijian He, Peixin Chen, Guangrun Wang, Guanbin Li, Philip HS Torr, and Liang Lin. Wildvidfit: Video virtual try-on in the wild via image-based controlled diffusion models. In *European Conference on Computer Vision*, pages 123–139. Springer, 2024. 2
- [16] Edward J Hu, Yelong Shen, Phillip Wallis, Zeyuan Allen-Zhu, Yuanzhi Li, Shean Wang, Lu Wang, Weizhu Chen, et al. Lora: Low-rank adaptation of large language models. *ICLR*, 1(2):3, 2022. 4, 12
- [17] Boyuan Jiang, Xiaobin Hu, Donghao Luo, Qingdong He, Chengming Xu, Jinlong Peng, Jiangning Zhang, Chengjie Wang, Yunsheng Wu, and Yanwei Fu. Fitdit: Advancing the authentic garment details for high-fidelity virtual try-on. *arXiv preprint arXiv:2411.10499*, 2024. 6
- [18] Jianbin Jiang, Tan Wang, He Yan, and Junhui Liu. Clothformer: Taming video virtual try-on in all module. In *Proceedings of the IEEE/CVF Conference on Computer Vision and Pattern Recognition*, pages 10799–10808, 2022. 7, 12
- [19] Jeongho Kim, Guojung Gu, Minhoo Park, Sunghyun Park, and Jaegul Choo. Stableviton: Learning semantic correspondence with latent diffusion model for virtual try-on. In *Proceedings of the IEEE/CVF conference on computer vision and pattern recognition*, pages 8176–8185, 2024. 7
- [20] Weijie Kong, Qi Tian, Zijian Zhang, Rox Min, Zuozhuo Dai, Jin Zhou, Jiangfeng Xiong, Xin Li, Bo Wu, Jianwei Zhang, et al. Hunyuanvideo: A systematic framework for large video generative models. *arXiv preprint arXiv:2412.03603*, 2024. 2, 12
- [21] Black Forest Labs. Flux. <https://github.com/black-forest-labs/flux>, 2024. 12
- [22] Guangyuan Li, Siming Zheng, Hao Zhang, Jinwei Chen, Junsheng Luan, Binkai Ou, Lei Zhao, Bo Li, and Peng-Tao Jiang. Magictryon: Harnessing diffusion transformer

- for garment-preserving video virtual try-on. *arXiv preprint arXiv:2505.21325*, 2025. 2, 4, 5, 7, 8, 12, 13
- [23] Junnan Li, Dongxu Li, Silvio Savarese, and Steven Hoi. Blip-2: bootstrapping language-image pre-training with frozen image encoders and large language models. In *Proceedings of the 40th International Conference on Machine Learning*. JMLR.org, 2023. 4
- [24] Peike Li, Yunqiu Xu, Yunchao Wei, and Yi Yang. Self-correction for human parsing. *IEEE Transactions on Pattern Analysis and Machine Intelligence*, 44(6):3260–3271, 2020. 3, 4, 13
- [25] Siqi Li, Zhengkai Jiang, Jiawei Zhou, Zhihong Liu, Xiaowei Chi, and Haoqian Wang. Realvvt: Towards photorealistic video virtual try-on via spatio-temporal consistency. *CoRR*, abs/2501.08682, 2025. 2
- [26] Haotian Liu, Chunyuan Li, Qingyang Wu, and Yong Jae Lee. Visual instruction tuning. *Advances in neural information processing systems*, 36:34892–34916, 2023. 12
- [27] Davide Morelli, Matteo Fincato, Marcella Cornia, Federico Landi, Fabio Cesari, and Rita Cucchiara. Dress code: High-resolution multi-category virtual try-on. In *Proceedings of the IEEE/CVF conference on computer vision and pattern recognition*, pages 2231–2235, 2022. 6, 7
- [28] Davide Morelli, Alberto Baldrati, Giuseppe Cartella, Marcella Cornia, Marco Bertini, and Rita Cucchiara. Ladi-vton: Latent diffusion textual-inversion enhanced virtual try-on. In *Proceedings of the 31st ACM international conference on multimedia*, pages 8580–8589, 2023. 7
- [29] Hung Nguyen, Quang Qui-Vinh Nguyen, Khoi Nguyen, and Rang Nguyen. Swifttry: Fast and consistent video virtual try-on with diffusion models. In *Proceedings of the AAAI Conference on Artificial Intelligence*, pages 6200–6208, 2025. 2
- [30] William Peebles and Saining Xie. Scalable diffusion models with transformers. In *Proceedings of the IEEE/CVF international conference on computer vision*, pages 4195–4205, 2023. 2
- [31] Adam Polyak, Amit Zohar, Andrew Brown, Andros Tjandra, Animesh Sinha, Ann Lee, Apoorv Vyas, Bowen Shi, Chih-Yao Ma, Ching-Yao Chuang, et al. Movie gen: A cast of media foundation models. *arXiv preprint arXiv:2410.13720*, 2024. 12
- [32] Robin Rombach, Andreas Blattmann, Dominik Lorenz, Patrick Esser, and Björn Ommer. High-resolution image synthesis with latent diffusion models. In *Proceedings of the IEEE/CVF conference on computer vision and pattern recognition*, pages 10684–10695, 2022. 8, 12
- [33] Olaf Ronneberger, Philipp Fischer, and Thomas Brox. U-net: Convolutional networks for biomedical image segmentation. In *International Conference on Medical image computing and computer-assisted intervention*, pages 234–241. Springer, 2015. 2, 12
- [34] Du Tran, Lubomir Bourdev, Rob Fergus, Lorenzo Torresani, and Manohar Paluri. Learning spatiotemporal features with 3d convolutional networks. In *Proceedings of the IEEE international conference on computer vision*, pages 4489–4497, 2015. 12
- [35] Team Wan, Ang Wang, Baole Ai, Bin Wen, Chaojie Mao, Chen-Wei Xie, Di Chen, Feiwu Yu, Haiming Zhao, Jianxiao Yang, et al. Wan: Open and advanced large-scale video generative models. *arXiv preprint arXiv:2503.20314*, 2025. 2, 8, 12
- [36] Yuanbin Wang, Weilun Dai, Long Chan, Huanyu Zhou, Aixi Zhang, and Si Liu. Gpd-vvto: Preserving garment details in video virtual try-on. In *Proceedings of the 32nd ACM International Conference on Multimedia*, pages 7133–7142, 2024. 2, 7
- [37] Zhou Wang, Alan C Bovik, Hamid R Sheikh, and Eero P Simoncelli. Image quality assessment: from error visibility to structural similarity. *IEEE transactions on image processing*, 13(4):600–612, 2004. 13
- [38] Jay Zhangjie Wu, Yixiao Ge, Xintao Wang, Stan Weixian Lei, Yuchao Gu, Yufei Shi, Wynne Hsu, Ying Shan, Xiaohu Qie, and Mike Zheng Shou. Tune-a-video: One-shot tuning of image diffusion models for text-to-video generation. In *Proceedings of the IEEE/CVF international conference on computer vision*, pages 7623–7633, 2023. 12
- [39] Saining Xie, Ross Girshick, Piotr Dollár, Zhuowen Tu, and Kaiming He. Aggregated residual transformations for deep neural networks. In *Proceedings of the IEEE conference on computer vision and pattern recognition*, pages 1492–1500, 2017. 13
- [40] Yuhao Xu, Tao Gu, Weifeng Chen, and Arlene Chen. Ootd-iffusion: Outfitting fusion based latent diffusion for controllable virtual try-on. In *Proceedings of the AAAI Conference on Artificial Intelligence*, pages 8996–9004, 2025. 3, 7
- [41] Zhengze Xu, Mengting Chen, Zhao Wang, Linyu Xing, Zhonghua Zhai, Nong Sang, Jinsong Lan, Shuai Xiao, and Changxin Gao. Tunnel try-on: Excavating spatial-temporal tunnels for high-quality virtual try-on in videos. In *Proceedings of the 32nd ACM International Conference on Multimedia*, pages 3199–3208, 2024. 2, 12
- [42] Zhuoyi Yang, Jiayan Teng, Wendi Zheng, Ming Ding, Shiyu Huang, Jiazheng Xu, Yuanming Yang, Wenyi Hong, Xiaohan Zhang, Guanyu Feng, et al. Cogvideox: Text-to-video diffusion models with an expert transformer. *arXiv preprint arXiv:2408.06072*, 2024. 12
- [43] Han Zhang, Ian Goodfellow, Dimitris Metaxas, and Augustus Odena. Self-attention generative adversarial networks. In *International conference on machine learning*, pages 7354–7363. PMLR, 2019. 12
- [44] Richard Zhang, Phillip Isola, Alexei A Efros, Eli Shechtman, and Oliver Wang. The unreasonable effectiveness of deep features as a perceptual metric. In *Proceedings of the IEEE conference on computer vision and pattern recognition*, pages 586–595, 2018. 13
- [45] Jun Zheng, Jing Wang, Fuwei Zhao, Xujie Zhang, and Xiaodan Liang. Dynamic try-on: Taming video virtual try-on with dynamic attention mechanism. *arXiv preprint arXiv:2412.09822*, 2024. 12
- [46] Xiaojing Zhong, Zhonghua Wu, Taizhe Tan, Guosheng Lin, and Qingyao Wu. Mv-ton: Memory-based video virtual try-on network. In *Proceedings of the 29th ACM International Conference on Multimedia*, pages 908–916, 2021. 7, 12
- [47] Tongchun Zuo, Zaiyu Huang, Shuliang Ning, Ente Lin, Chao Liang, Zerong Zheng, Jianwen Jiang, Yuan Zhang,

Mingyuan Gao, and Xin Dong. Dreamvvt: Mastering realistic video virtual try-on in the wild via a stage-wise diffusion transformer framework. *arXiv preprint arXiv:2508.02807*, 2025. [2](#), [4](#), [7](#), [12](#)

Appendix

A. Related Work

Video virtual try-on (VVT) aims to replace a person’s clothing with a target garment while preserving the spatiotemporal consistency of the video, i.e., the generated results should ensure a consistent appearance of the target garment across frames, align seamlessly with the person’s pose and motion, and maintain the rest of the scene without distortion.

GAN-based methods. Earlier works adopt GAN-based generators for VVT [6, 11, 18, 46]. For instance, FWGAN [11], as the first attempt, introduces an optical flow-guided warping GAN to deform the target garment and align it with the character’s body, thereby generating coherent video frames. MV-TON [46] leverages memory refinement to enhance details from previously generated frames. ClothFormer [18] employs a dual-stream transformer to address the temporal consistency of warped input sequences.

Diffusion model-based methods. Inspired by the advances of diffusion models in video generation [2, 20, 35], the latest studies [9, 13, 41, 45] have delved deeper into developing diffusion model-based frameworks for solving VVT tasks. For instance, ViVid [13] and Tunnel Try-on [41] incorporate a clothing reference branch into the stable diffusion framework to inject appearance features of the target garment. They further introduce temporal modeling strategies to ensure temporal coherence across frames, achieving visually plausible and temporally consistent video generation. However, these pioneering methods treat spatial and temporal information separately and are limited to low-quality outputs due to the restricted expressive capacity of U-Net [33] backbones.

DiT-based methods. To achieve superior realism and fine-grained detail preservation in virtual try-on applications, subsequent efforts [9, 22, 47] have explored diffusion transformer (DiT)-based diffusion models. These methods typically adopt a dual-branch architecture, where a dedicated clothing branch encodes appearance features, which are then combined with other input conditions and fed into DiT blocks for garment transfer. The DiT structure facilitates the joint modeling of spatial and temporal consistency. Furthermore, additional interaction modules are incorporated into the DiT blocks to better preserve garment details.

Despite the significant advancements of these DiT-based methods, they still suffer from limitations in fully capturing garment dynamics and background details. Furthermore, the introduction of additional components into DiT blocks often leads to increased complexity and computational overhead. Finally, the broader applicability of the DiT architecture remains constrained by the limited scale of publicly available datasets for virtual try-on tasks. Our KeyTailor of-

fers a more lightweight solution that improves garment fidelity and background consistency by injecting keyframe-driven details without explicitly modifying the DiT architecture. In addition, we curate a large-scale, high-quality dataset ViT-HD, to address the issue of data scarcity.

Diffusion Model for Video Generation With the continuous development of diffusion-based image synthesis techniques [12, 21, 32], numerous frameworks have been proposed to extend diffusion models to the field of video generation [2, 20, 35]. The architectures of diffusion-based generative methods can be broadly categorized into two types: U-Net architecture and Transformer architecture. Stable Video Diffusion [2] extends Stable Diffusion [32] by incorporating temporal modeling mechanisms such as temporal attention [38] and 3D convolutions [34], thereby enhancing frame consistency and content coherence across video sequences. Wan employs a 3D causal variational autoencoder (VAE) [31, 42] to capture complex temporal dynamics and extends the Diffusion Transformer (DiT) architecture from the image domain to the video domain, thereby achieving high-quality and temporally consistent video synthesis.

B. Preliminary

Diffusion Transformers (DiTs) have revolutionized video generation with their strong expressive power, ensuring higher fidelity and alignment in video synthesis. Wan [35] represents the current state-of-the-art among open-source video diffusion models, offering broad practical value. It adopts an LLaVA-style architecture [26], consisting of a variational autoencoder (VAE), a text encoder umT5 [10], and a DiT backbone. The core DiT network is composed of a patchifying module, multiple Transformer blocks, and an unpatchifying module. To ensure effective instruction following in long-context scenarios, Wan alternates between cross-attention and self-attention mechanisms [5, 43].

Wan processes noisy video tokens $x_0 \in \mathbb{R}^{N \times d}$ and text condition embeddings $ctxt \in \mathbb{R}^{M \times d}$, where $x_0 \sim \mathcal{N}(0, I)$, d denotes the embedding dimension, and N and M represent the number of video and text tokens, respectively. Leveraging flow matching, Wan circumvents iterative velocity prediction. In flow matching, given a latent representation of the target video x_1 , a random noise sample x_0 , and a timestep $t \in [0, 1]$ sampled from a logit-normal distribution, the linear interpolation x_t between x_0 and x_1 is used as the training input:

$$x_t = tx_1 + (1 - t)x_0. \quad (A1)$$

The corresponding ground truth velocity field is:

$$v_t = \frac{dx_t}{dt} = x_1 - x_0. \quad (A2)$$

Low-Rank Adaptation (LoRA) [16] is a parameter-efficient finetuning technique that introduces low-rank ma-

trices to adapt pretrained models without directly updating the original weights. Given a pre-trained weight matrix $W_0 \in \mathbb{R}^{d \times k}$, LoRA approximates the updated weight as:

$$W = W_0 + \Delta W = W_0 + AB^T, \quad (\text{A3})$$

where $A \in \mathbb{R}^{d \times r}$ and $B \in \mathbb{R}^{k \times r}$ are trainable low-rank matrices with rank $r \ll \min(d, k)$. This low-rank decomposition significantly reduces the number of trainable parameters, enabling efficient adaptation while preserving the performance of the original model.

C. Score Definition

In this section, we provide the definitions of the score functions used in our work, i.e., motion difference score ($S_m(f)$), garment-area ratio score ($S_r(f)$), and background integrity score ($S_{bg}(f)$).

The motion difference score is used to quantify the discrepancy between the motion of a given frame and that of the anchor frames, and is defined as:

$$S_m(f) = \min_{f_a \in F_{anc}} (\cos(D(f), D(f_a))), \quad (\text{A4})$$

where $\cos(\cdot, \cdot) \in [0, 1]$. A lower value indicates a larger difference in skeleton direction.

The garment-area ratio score measures the proportion of a frame occupied by the garment, and its formulation is given as:

$$S_r(f) = \frac{\text{area}(\text{segment-cloth}(f))}{\text{area}(f)}. \quad (\text{A5})$$

Here, ‘‘segment-cloth’’ denotes the segmentation operation that extracts the garment area from the frame, implemented by using HumanParsing [24].

Similarly, the background integrity score measures the clarity and proportion of the preserved background, and is calculated as:

$$S_{bg}(f) = \text{Background Ratio}(f) \times \text{Clarity}(f), \quad (\text{A6})$$

where the background ratio is:

$$\text{Background Ratio}(f) = \frac{\text{area}(\text{segment-background}(f))}{\text{area}(f)}. \quad (\text{A7})$$

Specifically, the segment-background(f) is accomplished via HumanParsing [24], which first extracts the human region, and the background is then computed as

$$\text{segment-background}(f) = f \odot (1 - \text{segment-human}(f)). \quad (\text{A8})$$

And the clarity for frame f is computed as:

$$\text{Clarity}(f) = \left(\frac{|\{E(x, y) > T\}|}{|\{\text{background pixels}\}|} \right) \times \left(\frac{1}{255} \cdot \frac{\sum_{E(x, y) > T} E(x, y)}{|\{E(x, y) > T\}|} \right), \quad (\text{A9})$$

where E is the Sobel edge map of the background image, T is a fixed threshold (default 50). The first term denotes the edge density, and the second term represents the normalized average gradient strength.

D. Metrics

Following previous works [4, 14, 37, 44], we adopt three widely used metrics to evaluate video generation quality: SSIM, LPIPS, and VFID. SSIM measures the structural similarity between generated and reference videos, LPIPS captures perceptual differences between image pairs, and VFID assesses both temporal consistency and overall video quality, where I3D [4] and ResNeXt [39] are different backbone models. For image virtual try-on, we additionally use FID and KID, along with SSIM and LPIPS [22]. Herein, FID and KID measure the similarity between the distributions of two images.

E. Training Details

As shown in Fig. 4, finetuning is applied to the LoRA parameters added to the DiT blocks, the single-image try-on model, and the parameters of the mask guider and pose guider. All of these are initialized from pre-trained weights, while the remaining modules are kept frozen. The formulations of the LoRA weights for finetuning image virtual try-on are shown as follows:

$$\begin{aligned} Q_{Img} &= W_{Q,I} + A_{Q,I}B_{Q,I}^\top, \\ K_{Img} &= W_{K,I} + A_{K,I}B_{K,I}^\top, \\ V_{Img} &= W_{V,I} + A_{V,I}B_{V,I}^\top, \end{aligned} \quad (\text{A10})$$

Similarly, the LoRA weights for finetuning DiT in our Key-Tailor are defined as:

$$\begin{aligned} Q_{DiT} &= W_{Q,D} + A_{Q,D}B_{Q,D}^\top, \\ Q_{key} &= Q_{DiT} + A_{key}B_{key}^\top \cdot L_{avg-key}^\top, \\ K_{DiT} &= W_{K,D} + A_{K,D}B_{K,D}^\top, \\ V_{DiT} &= W_{V,D} + A_{V,D}B_{V,D}^\top, \end{aligned} \quad (\text{A11})$$

where W_* denotes the pre-trained weight matrix of the original projection layers, and A_* represents a low-rank trainable matrix with rank $r \ll \min(d, k)$. Q_{key} corresponds to the keyframe. This parameter-efficient adaptation enables dynamic modulation of attention mechanisms while preserving the original model capacity. We further apply LoRA to the linear transformations in the feed-forward network (FFN), where each weight matrix W_{F0} is similarly parameterized as:

$$W_F = W_F + A_FB_F^\top. \quad (\text{A12})$$

This extension allows for lightweight finetuning across both attention and MLP components of the diffusion transformer.

By leveraging flow matching to maintain equivalence with the maximum likelihood objective, the model is trained to learn the true velocity. The overall training objective \mathcal{L} is defined as:

$$\mathcal{L} = \mathbb{E}_{c_{\text{txt}}, t, x_1, x_0} [\|u(x_t, L, c_{\text{txt}}, t; \theta) - v_t\|_2^2] \quad (\text{A13})$$

where $u(x_t, L, c_{\text{txt}}, t; \theta)$ denotes the velocity predicted by the model.

F. Settings of Ablation Study

In this section, we present the detailed settings of the ablation study in Sec 4.3.

- **w/o IKS:** Replace instruction-guided keyframe sampling with random sampling of three frames from the input video. This variant validates the effectiveness of the instruction-guided keyframe sampling module.
- **w/o $S_r(f)$:** Use only the motion-difference score $S_m(f)$ to guide keyframe selection, without incorporating user-instruction parsing, keeping the rest unchanged. This variant evaluates the contribution of instruction guidance.
- **w/o \mathcal{D} :** Directly use the first frame of the input video to generate garment latents, without incorporating keyframe-driven garment details, keeping the rest unchanged. This variant examines the role of the distillation component.
- **w/o Q_{key} :** Continue injecting \bar{L}_g into DiTs, but remove the keyframe-LoRA weight matrix Q_{key} , keeping the rest unchanged. This variant tests the importance of keyframe-aware LoRA adaptation.
- **w/o L_{key}^{bg} :** Use only the background features L_{bg} extracted from V_{agn} , without fusing keyframe-based background features, keeping the rest unchanged. This variant validates the role of collaborative background details optimization.
- **w/o Fusion:** Replace weighted fusion of background features with direct concatenation $\text{Concat}(L_m, L_{key}^{max-bg})$, keeping the rest unchanged. This variant examines the benefit of weighted fusion.
- **w/o CBDO:** We deactivate the entire collaborative background details optimization module, while keeping all other components unchanged. This variant evaluates the contribution of background detail refinement.
- **w/o GDDE:** We deactivate the entire garment dynamic details enhancement module, while keeping all other components unchanged. This variant validates the importance of enriching garment dynamics.
- **$F_{key} = 1$:** We restrict the keyframe set to only the first frame ($K = 1$) as input, while keeping all other settings unchanged. This variant evaluates the importance of using multiple keyframes.

Algorithm 1: Instruction-Guided Keyframe Sampling

```

Input:  $V_{\text{in}}$ : Input video (T frames, indices  $0 \sim T - 1$  with timestamps  $t_0 \sim t_{T-1}$ )
Ins: User instruction (e.g., "Show front/back of clothes, raise hand to display sleeves")
Params:  $K_{\text{max}}$  (max keyframes: 3 for short video, 6 for long video),  $w_1 = 0.3, w_2 = 0.2, w_3 = 0.3, w_4 = 0.2$  (weight coefficients),  $T_{\text{thres}}$  (temporal interval threshold: video duration/5),  $\text{Occlu}_{\text{thres}} = 0.2$  (garment occlusion threshold),  $\lambda = 0.5$  (skeleton difference weight)
Output:  $F_{\text{key}}$ : Selected keyframe list (length  $\leq K_{\text{max}}$ )
 $\text{View}_{\text{targets}}, \text{Action}_{\text{targets}} = \text{parse\_instruction}(\text{Ins})$ ;
 $F_{\text{anchor}} = []$ ;
for each view  $\in \text{View}_{\text{targets}}$  do
   $F_{\text{anchor}}.append(\text{generate\_standard\_pose}(\text{view}))$ ;
for each action  $\in \text{Action}_{\text{targets}}$  do
   $F_{\text{anchor}}.append(\text{generate\_standard\_pose}(\text{action}))$ ;
 $D_{\text{anchor}} = [\text{compute\_joint\_direction}(f) \mid f \in F_{\text{anchor}}]$ ;
 $S = []$ ;
for  $i = 0$  to  $T - 1$  do
   $f = V_{\text{in}}[i], t = \text{timestamp of } f$ ;
   $S_{\text{ins}} = \text{vlm\_score}(f, \text{Ins})$ ;
   $D_f = \text{compute\_joint\_direction}(f)$ ;
   $S_m = \min(\{\text{cosine\_distance}(D_f, d) \mid d \in D_{\text{anchor}}\})$ ;
   $\text{cloth\_mask} = \text{segment\_garment}(f)$ ;
   $S_{\text{cloth}} = \text{area}(\text{cloth\_mask}) / \text{area}(f)$ ;
   $\text{occlusion\_ratio} = \text{area}(\text{occluded\_region}(\text{cloth\_mask})) / \text{area}(\text{cloth\_mask})$ ;
  if  $\text{occlusion\_ratio} > \text{Occlu}_{\text{thres}}$  then
     $\text{Continue}$ ;
   $\text{initial\_score} = w_1 * S_{\text{ins}} + w_2 * (1 - S_m) + w_3 * S_{\text{cloth}} + w_4 * 1.0$ ;
   $S.append((i, t, \text{initial\_score}))$ ;
 $S_{\text{sorted}} = \text{sort}(S, \text{key} = \lambda x : x[2], \text{reverse}=\text{True})$ ;
 $\text{Idx}_{\text{key}} = [], T_{\text{selected}} = []$ ;
for each  $(\text{idx}, t, \text{score}) \in S_{\text{sorted}}$  do
  if  $|\text{Idx}_{\text{key}}| \geq K_{\text{max}}$  then
     $\text{Break}$ ;
  if  $T_{\text{selected}}$  is empty then
     $S_t = 1.0$ ;
  else
     $\text{min\_t\_dist} = \min(\{|t - t_s| \mid t_s \in T_{\text{selected}}\})$ ;
     $S_t = \text{min\_t\_dist} / T_{\text{thres}}$ ;
   $\text{final\_score} = \text{score} * S_t$ ;
  if  $\text{Idx}_{\text{key}}$  is empty then
     $\text{Idx}_{\text{key}}.append(\text{idx})$ ;
     $T_{\text{selected}}.append(t)$ ;
  else
     $\text{min\_score\_diff} = \min(\{|\text{final\_score} - S[\text{ik}][2]| \mid \text{ik} \in \text{Idx}_{\text{key}}\})$ ;
    if  $\text{min\_score\_diff} \geq 0.1$  and  $\text{min\_t\_dist} \geq T_{\text{thres}}$  then
       $\text{Idx}_{\text{key}}.append(\text{idx})$ ;
       $T_{\text{selected}}.append(t)$ ;
 $F_{\text{key}} = [V_{\text{in}}[\text{idx}] \mid \text{idx} \in \text{Idx}_{\text{key}}]$ ;
return  $F_{\text{key}}$ ;

```

G. Instruction-Guided Keyframe Sampling

The full procedure for instruction-guided keyframe sampling is provided in Algorithm 1.

H. Hyperparameter Studies

We conduct additional experiments to evaluate several key hyperparameters, including λ (Eq. 1), α (Eq. 3), and the number of keyframes. The experimental results are summarized in Tab. A1.

Table A1. Ablation studies on the ViT-HD dataset.

(a) Effect of λ			(b) Effect of α			(c) Effect of keyframe number		
λ	SSIM \uparrow	LPIPS \downarrow	α	SSIM \uparrow	LPIPS \downarrow	#KF	SSIM \uparrow	LPIPS \downarrow
0.1	0.9012	0.0683	0.1	0.8815	0.0362	1	0.8714	0.0678
0.2	0.9035	0.0571	0.2	0.8973	0.0378	2	0.8943	0.0512
0.3	0.9052	0.0486	0.3	0.9066	0.0397	3	0.9066	0.0397
0.4	0.9063	0.0429	0.4	0.9082	0.0435	4	0.9042	0.0419
0.5	0.9066	0.0397	0.5	0.9095	0.0489	5	0.9018	0.0445
0.6	0.9058	0.0435	0.6	0.9103	0.0557			
0.7	0.9031	0.0498	0.7	0.9108	0.0624			
0.8	0.8987	0.0576	0.8	0.9111	0.0689			
0.9	0.8924	0.0654	0.9	0.9113	0.0753			

Effect of λ and α . As shown in Tab. A1(a), the model achieves its best performance at $\lambda = 0.5$. In Eq. (1), λ controls the contribution of the garment-area ratio score $S_r(f)$ relative to the motion-difference term $S_m(f)$. When λ deviates from 0.5, the balance between motion cues and garment visibility becomes distorted, leading to reduced structural similarity (lower SSIM) and larger perceptual discrepancies (higher LPIPS). Similarly, from Tab. A1(b), the optimal value of α is 0.3. In Eq. (3), α determines how much the model relies on the general background latent code L_{bg} versus the frame representation L_{key}^{\max} that has the highest background completeness. Increasing α beyond 0.3 overweights L_{bg} , causing only minor improvements in structural similarity but a clear increase in perceptual distortion (higher LPIPS). This indicates that excessive emphasis on global background statistics harms perceptual fidelity, ultimately degrading overall visual quality.

Effect of keyframe number. To validate the choice of the keyframe number K , we conduct an ablation study in which all core modules (instruction-guided sampling, dynamic appearance distillation, and background co-optimization) are kept fixed while K is gradually increased. As shown in Table Tab. A1(c), the baseline setting of $K = 3$ yields the best performance (SSIM=0.9066, LPIPS=0.0397), as it effectively captures the user’s three essential requirements: front view, back view, and the hand-raising action. When $K = 1$, the model lacks sufficient multi-view and action cues, resulting in a large drop in both structural similarity (SSIM=0.8714) and perceptual fidelity (LPIPS=0.0678). Increasing to $K = 2$ still omits one required viewpoint or action, leading to incomplete appearance coverage and degraded consistency (SSIM=0.8943, LPIPS=0.0512). The optimal setting, $K = 3$, provides enough complementary visual information while avoiding redundancy. In contrast, using $K = 4$ or $K = 5$ introduces unnecessary or overlapping keyframes, which inject noise and feature conflicts into the fusion process, causing slight degradation (SSIM=0.9042/0.9018, LPIPS=0.0419/0.0445). Over-

all, setting $K = 3$ as the default provides a well-balanced design aligned with the instruction semantics and model behavior, ensuring sufficient motion and view coverage while enabling stable, high-quality generation.

I. More Qualitative Results

Fig. A1–Fig. A3 present additional visual comparisons between our KeyTailor and SOTA methods on the ViViD dataset, while Fig. A4–Fig. A6 show additional results on our self-collected ViT-HD. It is evident that KeyTailor produces more realistic and natural videos, capturing finer garment dynamics, preserving coherent background details, and maintaining temporal consistency across frames compared to existing methods.

J. Limitations

Our method still faces challenges in reliably handling complex garment–body interaction motions, largely due to the limited generative capacity of current pretrained models and the difficulty of accurately captioning fine-grained actions. We plan to further address and optimize these aspects in future work.

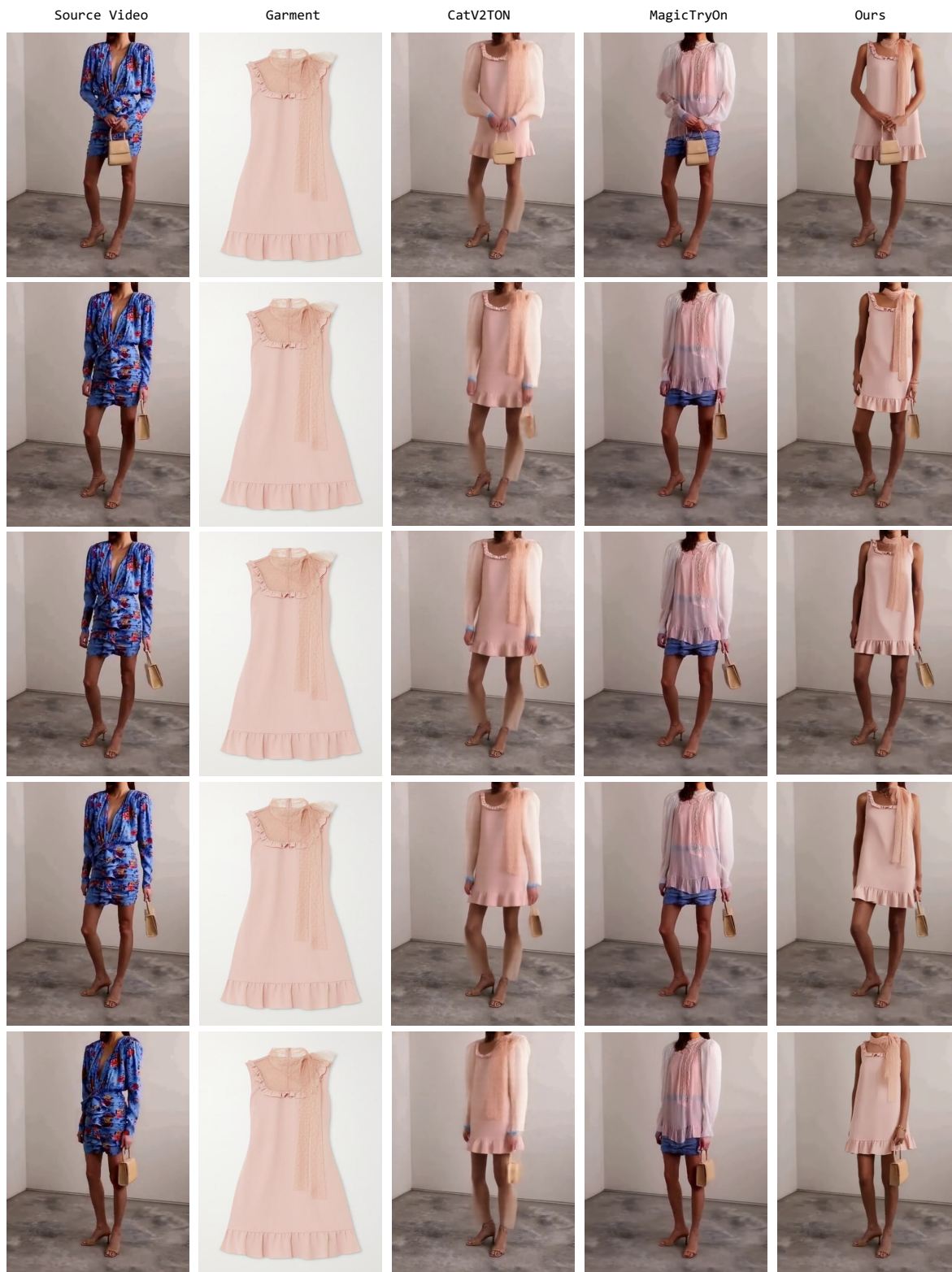


Figure A1. Additional qualitative comparison results on the ViViD dataset. Please zoom in for more details.



Figure A2. Additional qualitative comparison results on the ViViD dataset. Please zoom in for more details.

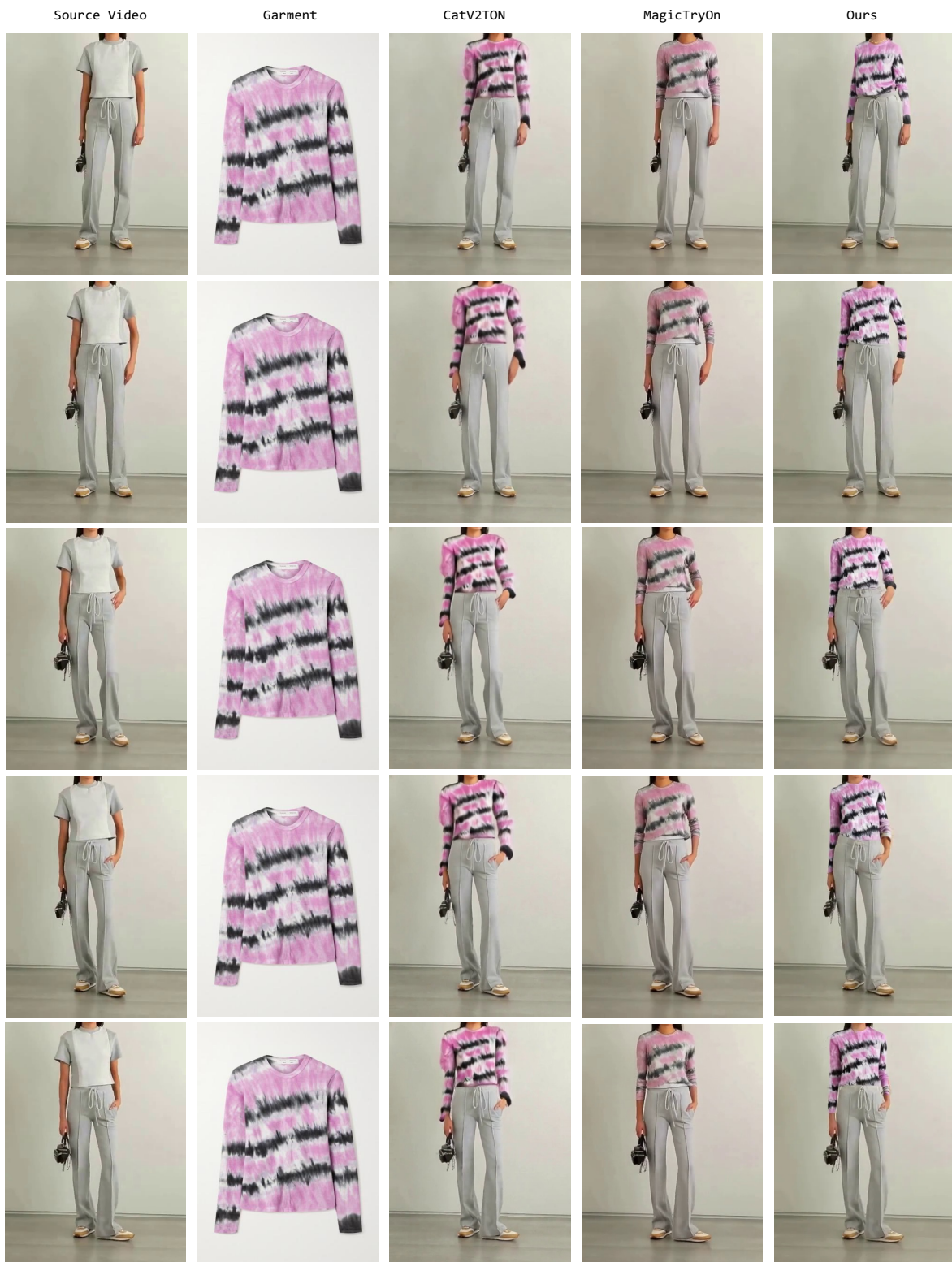


Figure A3. Additional qualitative comparison results on the ViViD dataset. Please zoom in for more details.



Figure A4. Additional qualitative comparison results on our ViT-HD dataset. Please zoom in for more details.



Figure A5. Additional qualitative comparison results on our ViT-HD dataset. Please zoom in for more details.



Figure A6. Additional qualitative comparison results on our ViT-HD dataset. Please zoom in for more details.